Chemical Engineering Journal 148 (2009) 459–472

Contents lists available at ScienceDirect

Chemical Engineering Journal

journal homepage: www.elsevier.com/locate/cej

Simulation of dye adsorption on hydrolyzed wheat straw in batch and fixed-bed systems

Fragiskos Batzias[a], Dimitris Sidiras[a,*], Elisabeth Schroeder[b], Christina Weber[b]

[a] Laboratory of Simulation of Industrial Processes, Department of Industrial Management and Technology, University of Piraeus, 80 Karaoli & Dimitriou St., GR 18534 Piraeus, Greece
[b] Institut fuer Kern- und Energietechnik, Forschungszentrum Karlsruhe GmbH, Postfach 3640, 76021 Karlsruhe, Germany

ARTICLE INFO

Article history:
Received 26 July 2006
Received in revised form
11 September 2008
Accepted 20 September 2008

Keywords:
Basic dyes
Adsorption
Wheat straw
Acid hydrolysis
Column

ABSTRACT

The simulation of batch and column kinetics of Methylene Blue and Red Basic 22 adsorption on mild acid hydrolyzed wheat straw was investigated, using untreated wheat straw as control, in order to examine its properties for potential use as a low cost adsorbent for wastewater dye removal. The BET surface area, the adsorption capacities (estimated according to Freundlich and Langmuir models), indicated that mild acid hydrolysis enhances significantly the adsorption properties of the original material. This enhancement can be attributed to the removal of the hemicelluloses during sulfuric acid treatment, resulting in the 'opening' of the pores of lignocellulosic matrix's structure and the increasing of the BET surface area.

1. Introduction

Inexpensive, locally available and effective materials could be used in place of commercial activated carbon for the removal of dyes in aqueous solutions. The environmental impact of the dyes present in the wastewater streams of many industrial sectors, such as dyeing, textile, paper, tannery and the paint industry, has drawn a lot of attention, emphasizing the necessity for their removal. Undoubtedly, low-cost adsorbents offer a lot of promising benefits for commercial purposes in the future. In particular, straw, a relatively abundant and inexpensive material, has been extensively investigated as an adsorbent for removing contaminants from water. Other adsorbent materials that have been studied include wood sawdust and other agricultural residues, untreated or treated in various ways [1–3].

Among the untreated materials that have been investigated, many agricultural residues, such as wheat straw, rice husk, corncobs and wood chips, have been used successfully to adsorb individual dyes and dye mixtures in textile effluent [4]. They are commonly used as an adsorbent, especially for basic dyes, with capacity varying according to the structure of the dye and the mesh size [5]. Removal of methylene blue and other basic dyes has been carried out using cedar sawdust [6], rubber-wood sawdust [7] coir pith, an unwanted by-product from the coir processing industry [8], banana/orange peels [9] and palm-fruit bunch particles [10,11].

Concentrated sulfuric acid- and formaldehyde-treated wheat straw and dilute acid-hydrolyzed charred straw were successfully used as adsorbents for a variety of dyes [2,12]. Cellulose-based anionic dye adsorbents have been prepared from agricultural residues (e.g. wheat straw) treated with cross-linked polyethylenimine [13] or cross-linked amphoteric starch [14]; also, carbonized agricultural wastes such as coir pith [15], cassava peel [9], bagasse [16] and kudzu [17] have been utilized successfully for the removal of dyes from aqueous solutions. Prehydrolyzed (with dilute sulphuric acid solution at 100 °C) beech sawdust [18] and calcium chloride treated (at 100 °C) beech sawdust [19] has been proven to be effective for basic dyes adsorption in batch and fixed-bed systems.

The suitability of a range of materials as dye adsorbents (e.g. activated carbons from bamboo dust, coconut shell, groundnut shell, rice husk and straw) is often established using (i) the kinetics of methylene blue adsorption during batch and continuous (column) processes [20] and (ii) the BET surface area.

In the present study, the BET surface area and the removal of chemical grade Methylene Blue and commercial Red Basic 22 by acid hydrolyzed wheat straw was studied using untreated wheat straw as control. The batch and column adsorption kinetics of the two dyes were used to estimate the adsorption capacity of the

* Corresponding author. Tel.: +30 104 142360; fax: +30 104 142366.
E-mail address: sidiras@unipi.gr (D. Sidiras).

1385-8947/$ – see front matter © 2008 Elsevier B.V. All rights reserved.
doi:10.1016/j.cej.2008.09.025

Nomenclature

a'_{KF}	intercept of the linear relation K_F vs. B
a'_N	intercept of the linear relation N vs. B
a'_{qm}	intercept of the linear relation q_m vs. B
a_B	intercept of the linear relation B vs. C_p
a_{KF}	intercept of the linear relation K_F vs. C_p
a_N	intercept of the linear relation N vs. C_p
a_{qm}	intercept of the linear relation q_m vs. C_p
b'_{KF}	slope of the linear relation K_F vs. B
b'_N	slope of the linear relation N vs. B
b'_{qm}	slope of the linear relation q_m vs. B
b_B	slope of the linear relation B vs. C_p
b_{KF}	slope of the linear relation K_F vs. C_p
b_N	slope of the linear relation N vs. C_p
b_{qm}	slope of the linear relation q_m vs. C_p
B	BET surface area ($m^2\,g^{-1}$)
B_0	value of B for acid hydrolysis reaction time $t = 0$ (at the beginning of the preheating period)
B_e	value of B for acid hydrolysis reaction time $t \to \infty$
c	intercept of the intra-particle diffusion equation
C	concentrations of Methylene Blue or Red Basic 22 in the bulk solution at time t in the case of batch adsorption process; also, the effluent concentration ($mg\,L^{-1}$) in the case of the column adsorption process
C_0	initial dye concentration ($mg\,L^{-1}$)
C_e	equilibrium concentration of the adsorbate ($mg\,L^{-1}$) for $t \to \infty$
C_i	influent concentration ($mg\,L^{-1}$) in the case of column adsorption process
C_p	removed polysaccharides, i.e. cellulose and hemicelluloses as dry weight of product of the original dry material (%, w/w)
C_{pe}	value of C_p for acid hydrolysis reaction time $t \to \infty$
E	adsorption activation energy
k	first order rate constant for the adsorption process (min^{-1}).
k_B	BET surface area kinetic constant (h^{-1})
k_N	kinetic constant (h^{-1})
k_p	hydrolysis first order rate kinetic constant (h^{-1})
k_p	intra-particle diffusion rate constant ($mg\,g^{-1}\,min^{-0.5}$)
k_{qm}	kinetic constant (h^{-1})
k_T	heating rate constant (h^{-1})
K	adsorption rate coefficient ($L\,mg^{-1}\,min^{-1}$) in the case of column adsorption process
K_F	Freundlich constant related to adsorption capacity
K_{F0}	value of K_F for acid hydrolysis reaction time $t = 0$ (at the beginning of the preheating period)
K_{Fe}	value of K_F for acid hydrolysis reaction time $t \to \infty$
K_{KF}	kinetic constant (h^{-1})
K_L	Langmuir constant related to the energy of adsorption ($L\,mg^{-1}$)
m	weight of the adsorbent used (g)
n	inverse of the slope of the Freundlich isotherm, it is related to adsorption intensity
N	adsorption capacity coefficient ($mg\,L^{-1}$) in the case of column adsorption process
N_0	value of N for acid hydrolysis reaction time $t = 0$ (at the beginning of the preheating period)
N_e	value of N for acid hydrolysis reaction time $t \to \infty$
p	frequency factor at the Arrhenius law (min^{-1})
q	amount adsorbed per unit mass of the adsorbent ($mg\,g^{-1}$)
q_m	Langmuir constant related the amount of dye adsorbed ($mg\,g^{-1}$) when the saturation is attained
q_{m0}	value of q_m for acid hydrolysis reaction time $t = 0$ (at the beginning of the preheating period)
q_{me}	value of q_m for acid hydrolysis reaction time $t \to \infty$
q_t	amounts of dye adsorbed per unit mass of the adsorbent (in $mg\,g^{-1}$) at time t
R_L	dimensionless constant called 'equilibrium parameter' or 'separation factor' expressing the essential characteristics of the Langmuir isotherm
SEE	standard error of estimate
t	adsorption or acid hydrolysis treatment time (in min or in h, respectively).
T	adsorption or acid hydrolysis treatment temperature (K)
T_0	acid hydrolysis reaction initial temperature (at the beginning of the preheating period), i.e. the value of T for $t = 0$
T_e	acid hydrolysis reaction final temperature, i.e. the value of T for $t \to \infty$
u	linear velocity (cm/min) in the case of column adsorption process
x	bed depth of the adsorption column (cm)

Greek symbols

$\alpha_1, \beta_1, \gamma_1, \delta_1, \varepsilon_1$	empirical parameters of the equation for the Freundlich parameter K_F as a function of pH

untreated and treated by mild acid-hydrolysis wheat straw. The effect of the hydrolysis time on the adsorption capacity and the BET surface area was also investigated. The results indicate that the acid hydrolyzed lignocellulosic material exhibits advanced adsorption properties and higher BET surface area values compared to the original material, enhanced by increasing the pretreatment time. Considering the abundance and low cost of the original material and the vast applicability of the treatment process proposed herein, the treated wheat straw could be an extremely cost-effective adsorbent for basic dyes.

2. Experimental

2.1. Materials development

The wheat straw used was obtained from the Greek region of Thessaly, as a suitable source for full-scale/industrial applications. The moisture of the material when received was 9% w/w. After grinding by a hummer mill and screening, the fraction with particle sizes between 0.2 and 0.8 mm was isolated as 'fine grinded wheat straw' and the fraction with particle sizes between 0.8 and 8 mm was isolated as 'coarse grinded wheat straw'. The chemical composition and the BET surface area of the raw material are presented in Table 1.

The mild acid hydrolysis process was performed in a 500-mL glass batch reactor, equipped with an internal thermocouple, immersed in a heating oil bath [21,22]. The mild acid hydrolysis final temperature was 100 °C; 1.8 M H_2SO_4 solution catalyzed the reaction at a liquid-to-solid ratio of 10:1 by mass. The reaction time was 0.5, 1, 2, 3, 4 and 5 h, plus 40 min the preheating period.

The composition of the pre-treated wheat straw (cellulose, hemicelluloses, lignin, etc. as dry weight of product % (w/w) of the

Table 1
Composition and BET surface area of the original and the hydrolyzed wheat straw.

Component	Composition (expressed as % (w/w) on a dry weight basis of the hydrolyzed material)						
	Original wheat straw	Wheat straw pre-treated with 1.8 M H_2SO_4 at 100 °C					
		0.5 h[a]	1 h[a]	2 h[a]	3 h[a]	4 h[a]	5 h[a]
Fine grinded wheat straw							
Cellulose[b]	36.2	50.6	53.0	52.1	51.0	47.9	47.3
Hemicelluloses	31.6	15.2	6.1	2.3	0.9	0.3	0.1
Acid-insoluble lignin	27.2	38.5	41.5	43.7	45.7	45.7	47.9
Ash	1.0	1.4	1.5	1.6	1.7	1.7	1.8
Extractives and others	4.0	5.7	6.1	6.4	6.7	6.7	7.0
BET surface area ($m^2\,g^{-1}$)	3.1	6.1	6.8	11.0	11.0	11.5	9.0
Coarse grinded wheat straw							
Cellulose[b]	37.0	49.6	52.0	51.1	50.0	46.9	46.4
Hemicelluloses	30.9	14.9	5.9	2.3	0.9	0.3	0.1
Acid-insoluble lignin	27.7	37.8	40.7	42.8	44.8	44.9	47.0
Ash	0.8	1.4	1.5	1.6	1.6	1.6	1.7
Extractives and others	3.6	5.6	6.0	6.3	6.6	6.6	6.9
BET surface area ($m^2\,g^{-1}$)	5.3	7.6	11.9	13.7	14.0	13.5	14.5

[a] Hydrolysis reaction time without including preheating time.
[b] Degree of crystallinity 80%.

pre-treated dry material) and the BET surface area values of the treated material are presented in Table 1.

2.2. Adsorption studies

Adsorption isotherms were derived from batch experiments. Following the batch procedure, accurately weighed quantities of adsorbent (0.5 g with particle sizes between 0.2 and 0.8 mm or 0.8 and 8 mm, respectively) were transferred into 0.8-L bottles, where 0.5 L of buffered (at pH 8) adsorbate solution were added. The Methylene Blue and Red Basic 22 initial concentrations were 1.4–14 mg L^{-1} and 3.2–32 mg L^{-1}, respectively. The bottles were sealed and mechanically tumbled for a period of 7 days at 23 °C. The resulting solution concentrations were determined and the equilibrium data from each bottle represented one point on the adsorption isotherm plots.

2.3. Kinetic studies

Adsorption rate batch experiments were conducted in a 2-L completely mixed glass reactor fitted with a twisted blade-type stirrer, operated at 600 rpm to keep the lignocellulosic material in suspension. The reactor, containing 1 L aquatic dye solution and 1 g adsorbent (with particle sizes between 0.2 and 0.8 mm or 0.8 and 8 mm), was placed into a water bath to keep temperature constant at the desired level (23 °C). The Methylene Blue and Red Basic 22 initial concentrations were 1.4–14 mg/L and 3.2–32 mg L^{-1}, respectively. The effect of stirring was studied in the range of 0–1000 rpm. The pH effect was studied in the range of 1.5–13 (the pH values of the dye solutions were adjusted using dilute H_2SO_4 or NaOH solutions, as appropriate).

2.4. Column studies

Fixed-bed up-flow adsorber studies were conducted in 10 cm × 2 cm and 20 cm × 2 cm glass columns filled with 10 and 20 g of fine grinded wheat straw or 5 and 10 g of coarse grinded wheat straw, respectively. The experimental set-up consisted of three parallel columns, fed by a multi-channel peristaltic pump at a constant flow rate, ranging from 5 to 15 mL min^{-1}. The Methylene Blue and Red Basic 22 influent concentrations were 14 and 32 mg L^{-1}, respectively. Interconnective tubing and fitting were made of polytetrafluoroethylene (PTFE). Effluent samples were analyzed to yield output concentration breakthrough curves.

2.5. Analytical techniques

The degree of crystallinity of wood cellulose was measured with the X-ray diffraction method proposed by Segal et al. [23]. Following the technique proposed by Saeman et al. [24], the lignocellulosic materials were hydrolyzed to glucose and reducing sugars in nearly quantitative yields; the filtrates were analyzed for glucose using the Glu-cinet test and for reducing sugars using the Somogyi technique [25]. Based on these results the cellulose and hemicelluloses contents of the adsorbents were estimated. Finally, the acid-insoluble lignin (Klason lignin) was determined according to the Tappi T222 om-88 method.

The BET (Brunauer, Emmet and Teller) surface area of the original and the pre-treated straw was measured from the N_2 adsorption isotherm with an 'Areameter II' (Juwe-Laborgeräte GmbH) sorptiometer in accordance with DIN 66132 [26]. Prior to this measurement, the samples were dried under vacuum at 150 °C overnight to clean the surface.

The concentrations of Methylene Blue and Red Basic 22 in the solution were obtained by measuring O.D. at 663 and 530 nm (λ_{max}) respectively, using a HACH DR4000U UV–vis spectrophotometer. The effect of the pH at the λ_{max} value for specifically severe conditions (pH > 12 and adsorption time t = 7 days) was taken into account.

3. Results and discussion

3.1. Simulation of the mild acid hydrolysis

Cellulose crystallinity, accessible surface area, protection by lignin, and cellulose sheathing by hemicelluloses all contribute to its resistance of biomass hydrolysis [27]. Dilute acid hydrolysis of cellulose and hemicelluloses produces glucose, xylose and degradation products as furfural. The hydrolysis is affected by temperature, concentration of acid and reaction time [28]. The detailed simulation of the mild acid hydrolysis process was performed using 'HYDROSTRAW', a simulation model for dilute acid hydrolysis of lignocellulosic materials [22], adapted to the wheat straw hydrolysis data presented herein. Cellulose fractions are hydrolyzed to water-soluble glucose, hemicelluloses are hydrolyzed to xylose and

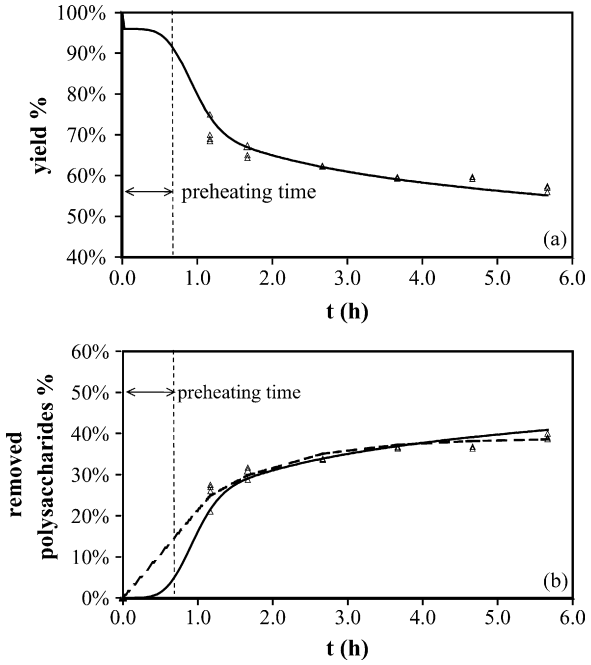

Fig. 1. Simulation of the (a) yield of the pre-treated wheat straw (dry weight of product % (w/w) of the original dry material) and (b) the removed polysaccharides (cellulose and hemicelluloses) fraction (dry weight of product % (w/w) of the original dry material) vs. the acid hydrolysis time (reaction final temperature: 100 °C; 1.8 M H_2SO_4 aquatic solution; liquid-to-solid ratio: 10:1 by mass).

acid-insoluble lignin fraction is not affected by mild acid hydrolysis.

Amorphous cellulose → glucose → degradation products.
Crystalline cellulose → glucose → degradation products.
Easily hydrolyzed hemicelluloses → xylose → degradation products.
Resistant to hydrolyzed hemicelluloses → xylose → degradation products.
Lignin → not hydrolyzed.

According to the simulation applied in the present work, more than 67% (w/w) of the amorphous cellulose, 16% (w/w) of the crystalline cellulose, 99.9% (w/w) of the easily hydrolyzed hemicelluloses and 99% (w/w) of the resistant to hydrolysis hemicelluloses were hydrolyzed at 5 h acid hydrolysis time (without including 40 min preheating period). The results for the yield of the pre-treated wheat straw (dry weight of product % (w/w) of the original dry material) vs. reaction time (t in hours) are given in Fig. 1a. The removed polysaccharides C_p (cellulose and hemicelluloses as dry weight of product % (w/w) of the original dry material) are given in Fig. 1b (solid line). The reaction temperature profile was simulated by the equation

$$T = T_e - (T_e - T_0)e^{-k_T t} \quad (1)$$

where T_e is the acid hydrolysis reaction final temperature, i.e. the value of T for $t \to \infty$, T_0 is the reaction initial temperature (at the beginning of the preheating period), i.e. the value of T for $t = 0$ and k_T is the heating rate constant in h^{-1}. The parameters were found by non-linear regression analysis, $T_e = 100$ °C, $T_0 = 10$ °C and $k_T = 0.038\ h^{-1}$.

Alternatively, the simulation of the removed polysaccharides, for reaction time including preheating period >(40 + 30)/60 = 1.17 h, can be approximately achieved by simple first order kinetics:

$$\frac{dC_p}{dt} = k(C_{pe} - C_p), \text{ which gives } C_p = C_{pe}(1 - e^{-k_p t}) \quad (2)$$

where C_{pe} is the value of C_p for $t \to \infty$, and k_p is the hydrolysis kinetic constant in h^{-1}. The value of C_p is zero for $t = 0$ (at the beginning of the preheating period). The C_{pe} was found to be approximately equal to the hemicelluloses and the amorphous cellulose quantity. The crystalline cellulose was not hydrolyzed at the conditions used herein. The k_p parameter value was found by non-linear regression analysis (Table 6). The alternative simulation results are shown by the dashed line in Fig. 1b.

3.2. Simulation of the BET surface area as affected by the mild acid hydrolysis

Introducing the surface area B (in $m^2\ g^{-1}$, measured by the BET method) as a variable, possibly depended on C_p, we observe an almost linear relation between them (Fig. 2b):

$$B = a_B + b_B C_p \quad (3)$$

The results from the fitting of Eq. (3) to the experimental data are given in Fig. 2a and the parameters' values are given in Table 6. The BET surface area is increasing linearly vs. the removed polysaccharides percentage (dry % (w/w) fraction of the original dry material) for both (fine and coarse grinded) wheat straw fractions.

By combining relations (2) and (3) we obtain Eq. (4), which simulates specific surface area B growth as a function of the mild acid hydrolysis processing time, including preheating period >(40 + 30)/60 = 1.17 h:

$$B = B_e - (B_e - B_0)e^{-k_B t} \quad (4)$$

where B_e is the value of B for hydrolysis time $t \to \infty$, B_0 is the value of B for $t = 0$ (at the beginning of the preheating period) and k_B is the BET surface area kinetic constant in h^{-1}. The parameters were found by non-linear regression analysis (Table 6). The solid line for

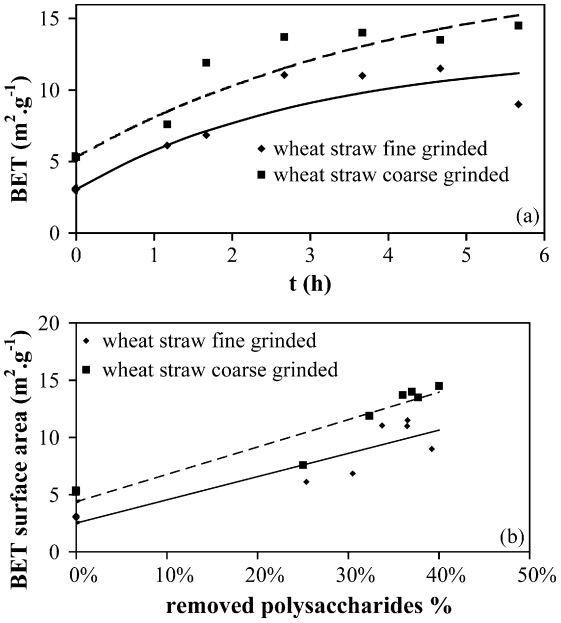

Fig. 2. Simulation of the BET surface area (a) vs. the acid hydrolysis time (reaction final temperature: 100 °C; 1.8 M H_2SO_4 aquatic solution; liquid-to-solid ratio: 10:1 by mass) and (b) vs. the removed polysaccharides (cellulose and hemicelluloses) fraction (dry weight of product % (w/w) of the original dry material) for the same hydrolysis reaction conditions. The solid lines correspond to the fine grinded wheat straw data and the dashed lines correspond to the coarse grinded wheat straw data.

the fine grinded wheat straw fraction and the dashed line for the coarse grinded wheat straw fraction are shown in Fig. 2a. By the assumption that $k_B = k_p$, then $B_e = a_B + b_B C_{pe}$ and $B_0 = B_e - b_b C_{pe}$.

The hemicelluloses content of the original wheat straw was significantly decreased by mild acid hydrolysis (the initial value of 31.6% (w/w) was decreased to 0.1% (w/w) of the hydrolyzed material after 5 h of treatment). The cellulose fraction decreased by its amorphous part (the initial value of 36.2% (w/w) was increased to 47.3% (w/w) of the hydrolyzed material but decreased to 26.9% (w/w) of the original material after 5 h of treatment) while the lignin quantity remained practically unchanged (according to the data in Table 1 combined with the Fig. 1 data). The efficient removal of the hemicelluloses (in the form of water soluble reducing sugars, e.g. xylose, etc.) and the amorphous part of cellulose (in the form of water soluble glucose) results in 'opening' of the pores of the structure of the lignocellulosic matrix [21,22]. This phenomenon has as a result the increasing the BET surface area of the material, which accounts for the advanced adsorption properties of the hydrolyzed materials over the untreated ones. Furthermore, the sulfuric acid treatment of the material possibly leads to the activation of the internal surface of wheat straw particles, thus increasing the number of active sites available for dye binding.

3.3. Adsorption isotherms

The comparison of the adsorption capacities of the untreated and pre-treated wheat straw samples was based on the Freundlich [29] and Langmuir [30] isotherm models, both commonly used for investigating the sorption of a variety of dyes on: straw [2], wood shavings [3], coir pith [8], banana/orange peels [9], palm-fruit bunch particles [11], dried kudzu [17], beech sawdust [18,19] and activated carbons [15,16,20,31–35].

The Freundlich [29] isotherm form is given by the following equation:

$$q = K_F (C_e)^{1/n} \tag{5}$$

where q is the amount adsorbed per unit mass of the adsorbent ($mg\,g^{-1}$), C_e is the equilibrium concentration of the adsorbate ($mg\,L^{-1}$) and K_F, n are the Freundlich constants related to adsorption capacity and intensity, respectively. The logarithmic form of Eq. (5) gives the following linearized expression:

$$\log q = \log K_F + \frac{1}{n} \log C_e \tag{6}$$

The Freundlich constants K_F and n were estimated by linear regression analysis from the experimental adsorption data obtained at 23 °C for Methylene Blue and Red Basic 22 (Table 2). In Fig. 3, methylene blue adsorption on the original and the 4 h hydrolyzed samples are given as an example for sake of comparison between them. The Freundlich parameter mean values are shown in Table 3. The parameter values estimated by non-linear regression gave only slightly lower S.E.E. (standard error of estimate) and were not significantly different in comparison with the values obtained by using the linearized expression (6). Further to simplicity of the algebraic determination of parameter-values (in comparison with the algorithmic procedures followed in non-linear approximations), the linearized expression provides values that can be directly compared with the results reported by most of the authors who have adopted this simpler approach.

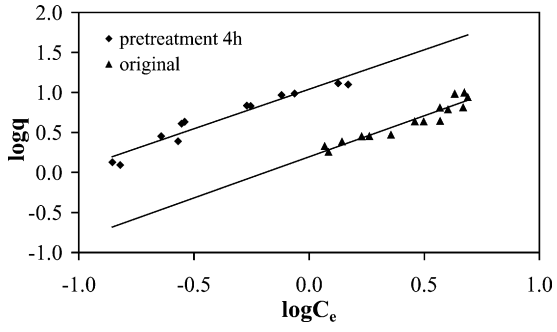

Fig. 3. Freundlich isotherms for the removal of methylene blue by adsorption on original and acid hydrolyzed for 4 h (the 40 min preheating period is not included) fine grinded wheat straw.

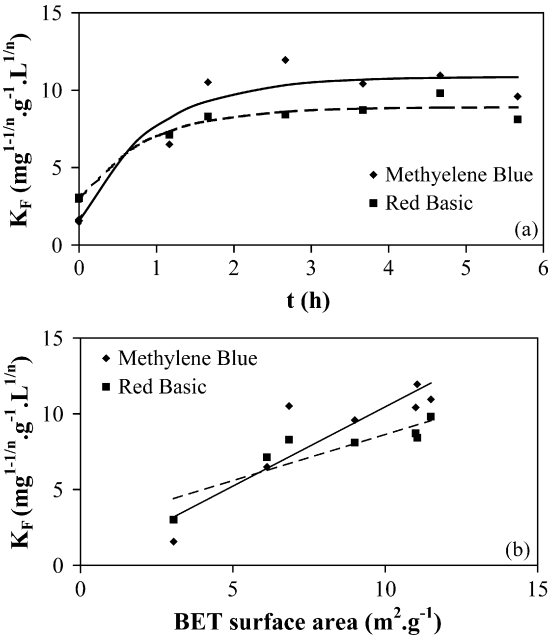

Fig. 4. Simulation of the Freundlich parameter values (K_F in $mg^{1-1/n}\,g^{-1}\,L^{1/n}$) vs. (a) the fine grinded wheat straw acid hydrolysis time (t in h) and (b) the corresponding BET surface area (B in $m^2\,g^{-1}$). The solid lines correspond to the methylene blue adsorption data and the dashed lines correspond to the Red Basic 22 adsorption data.

The K_F values estimated for the hydrolyzed samples were significantly higher, comparing to those of the untreated material for both dyes, indicating an increased adsorption capacity of the former; among pre-treated materials, higher values were obtained from the stronger hydrolyzed samples (higher hydrolysis reaction times). The goodness of fitting of the Freundlich equation to experimental data shows that the adsorbents' surface was most probably heterogeneous and capable for multiplayer adsorption.

Introducing the K_F parameter (in $mg^{1-1/n}\,g^{-1}\,L^{1/n}$), as a variable, possibly depended on C_p, we observe an almost linear relation between them:

$$K_F = a_{KF} + b_{KF} C_p \tag{7}$$

By combining relations (2) and (7) we obtain Eq. (8), which simulates K_F parameter (in $mg^{1-1/n}\,g^{-1}\,L^{1/n}$), growth as a function of the mild acid hydrolysis processing time, including preheating period >(40 + 30)/60 = 1.17 h:

$$K_F = K_{Fe} - (K_{Fe} - K_{F0}) e^{-k_{KF} t} \tag{8}$$

where K_{Fe} is the value of K_F for $t \to \infty$, K_{F0} is the value of K_F for $t = 0$ (at the beginning of the preheating period) and k_{KF} is the kinetic constant in h^{-1}. The parameters were found by non-linear regression analysis (Table 6). The solid line for the methylene blue absorption and the dashed line for the Red Basic 22 adsorption on the fine grinded wheat straw fraction are presented in Fig. 4a. Assuming that $k_{KF} = k_p$ then $K_{Fe} = a_{KF} + b_{KF} C_{pe}$, and $K_{F0} = K_{Fe} - b_{KF} C_{pe}$.

Table 2
The Freundlich parameters of adsorption isotherms.

Parameter	Original wheat straw	Wheat straw pre-treated with 1.8 M H_2SO_4 at 100 °C					
		0.5 h[a]	1 h[a]	2 h[a]	3 h[a]	4 h[a]	5 h[a]
Fine grinded wheat straw							
Methylene Blue							
K_F	1.57	6.50	10.52	11.95	10.42	10.95	9.59
n	0.97	1.30	1.37	1.33	1.09	1.01	1.40
Correlation coefficient (R)	0.9511	0.8762	0.8110	0.9686	0.9615	0.9683	0.9903
S.E.E. ($mg\,g^{-1}$)	1.06	1.15	1.24	1.04	1.05	1.42	1.39
Red Basic 22							
K_F	3.02	7.13	8.30	8.42	8.72	9.81	8.12
n	1.28	1.28	1.27	1.44	1.33	1.60	1.22
Correlation coefficient (R)	0.9251	0.9449	0.8881	0.9589	0.9871	0.8750	0.9820
S.E.E. ($mg\,g^{-1}$)	4.14	4.05	4.31	3.99	3.88	6.30	3.61
Coarse grinded wheat straw							
Methylene Blue							
K_F	2.68	8.06	18.27	14.82	13.26	12.86	15.45
n	1.66	1.62	1.43	1.64	1.39	1.19	1.35
Correlation coefficient (R)	0.9321	0.8586	0.7948	0.9492	0.9423	0.9489	0.9705
S.E.E. ($mg\,g^{-1}$)	1.08	1.17	1.27	1.06	1.07	1.45	1.42
Red Basic 22							
K_F	5.17	8.85	14.43	10.44	11.09	11.52	13.07
n	1.31	1.59	1.76	1.79	1.69	1.50	1.57
Correlation coefficient (R)	0.9066	0.9260	0.8704	0.9397	0.9673	0.8575	0.9624
S.E.E. ($mg\,g^{-1}$)	4.22	4.13	4.40	4.07	3.96	5.14	3.69

[a] Hydrolysis reaction time without including preheating time.

Alternatively, the same Eq. (8) comes from the combination of Eq. (3) with the following equation:

$$K_F = a'_{KF} + b'_{KF}B \quad (9)$$

by the assumption that $k_{KF} = k_B$. In this case $K_{Fe} = a'_{KF} + b'_{KF}B_e$, and $K_{F0} = K_{Fe} - b'_{KF}(B_e - B_0)$.

The results from the fitting of Eq. (9) to the experimental data are given in Fig. 4b (the solid line for the methylene blue absorption and the dashed line for the Red Basic 22 adsorption on the fine

Table 3
The Langmuir parameters of adsorption isotherms.

Parameter	Original wheat straw	Wheat straw pre-treated with 1.8 M H_2SO_4 at 100 °C					
		0.5 h[a]	1 h[a]	2 h[a]	3 h[a]	4 h[a]	5 h[a]
Fine grinded wheat straw							
Methylene Blue							
q_m ($mg\,g^{-1}$)	2.23	12.65	19.44	19.46	17.87	20.41	16.21
K_L ($L\,mg^{-1}$)	0.758	1.086	0.976	1.185	0.786	0.663	0.974
Correlation coefficient (R)	0.9652	0.7491	0.7075	0.9581	0.9568	0.9795	0.9546
S.E.E. ($mg\,g^{-1}$)	1.20	1.55	1.64	1.21	1.33	1.10	1.46
R_L[b]	0.086	0.062	0.068	0.057	0.083	0.097	0.068
Red Basic 22							
q_m ($mg\,g^{-1}$)	23.4	45.4	43.2	55.8	72.7	54.7	67.8
K_L ($L\,mg^{-1}$)	0.190	0.237	0.233	0.171	0.106	0.211	0.138
Correlation coefficient (R)	0.7347	0.9273	0.8932	0.9532	0.9949	0.8814	0.9749
S.E.E. ($mg\,g^{-1}$)	5.40	6.96	7.00	5.44	5.99	4.95	6.55
R_L[c]	0.141	0.116	0.118	0.154	0.227	0.129	0.185
Coarse grinded wheat straw							
Methylene Blue							
q_m ($mg\,g^{-1}$)	3.82	15.69	33.78	24.13	22.74	23.96	26.12
K_L ($L\,mg^{-1}$)	1.30	1.35	1.02	1.47	1.00	0.78	0.94
Correlation coefficient (R)	0.9459	0.7341	0.6933	0.9389	0.9377	0.9599	0.9355
S.E.E. ($mg\,g^{-1}$)	1.26	1.62	1.63	1.27	1.40	1.16	1.53
R_L[b]	0.052	0.050	0.066	0.046	0.067	0.084	0.071
Red Basic 22							
q_m ($mg\,g^{-1}$)	40.00	56.28	75.16	69.16	92.52	64.25	109.24
K_L ($L\,mg^{-1}$)	0.20	0.29	0.32	0.21	0.14	0.20	0.18
Correlation coefficient (R)	0.7714	0.9087	0.8754	0.9341	0.9750	0.8637	0.9554
S.E.E. ($mg\,g^{-1}$)	5.56	7.17	6.85	5.60	6.17	5.10	6.75
R_L[c]	0.138	0.096	0.088	0.128	0.188	0.136	0.149

[a] Hydrolysis reaction time without including preheating time.
[b] The R_L values for Methylene Blue adsorption are calculated for $C_0 = 14\,mg\,L^{-1}$.
[c] The R_L values fro Red Basic 22 adsorption are calculated for $C_0 = 32\,mg\,L^{-1}$.

grinded wheat straw fraction) and the parameters' values are given in Table 6. The K_F values are increasing linearly vs. BET surface area increasing for both (fine and coarse grinded) wheat straw fractions.

The Langmuir [30] isotherm equation is based on the following 'pseudo-monolayer' adsorption model.

$$\frac{1}{q} = \left(\frac{1}{q_m}\right) + \left(\frac{1}{K_L q_m}\right)\left(\frac{1}{C_e}\right) \quad (10)$$

where K_L is the Langmuir constant related to the energy of adsorption ($L\,mg^{-1}$) and q_m the amount of dye adsorbed ($mg\,g^{-1}$) when saturation is attained. The name 'pseudo-monolayer' is justified by a replacement of the original concept 'monolayer capacity' with 'saturation' as the upper limit for the amount of the adsorbed substance, implying a corresponding change in the adsorption driving force, which is the difference $q - q_t$, where q and q_t are the amounts of dye adsorbed per unit mass of the adsorbent material (in $mg\,g^{-1}$) at equilibrium time (∞) and adsorption time t, respectively. If the isotherm experimental data approximates the Langmuir equation, the parameters K_L and q_m can be obtained by plotting $1/q$ vs. $1/C_e$. Table 3 presents the estimated parameter-values for the data gathered in the present study. The adsorption capacities (q_m) obtained for untreated wheat straw were lower than the values for the hydrolyzed samples. The superiority of the more hydrolyzed sample over the less pre-treated ones is confirmed in the case of Methylene Blue and Red Basic 22 experiments, respectively. The goodness of fitting of the Langmuir's adsorption model to the present data is lower than the Freundlich's model, as shown by the high S.E.E. Nevertheless the validity and use of both models (although with different S.E.E.-values) provides us with reliable parameter-values which can be used in the same knowledge base (KB) together with the results reported by other authors, who have worked on only one of these models; this provision is a prerequisite for an inference engine to perform data mining (for comparing results from various sources) in such a KB according to the principle of consistency.

The essential characteristics of the Langmuir [30] isotherm can be described by a dimensionless constant called 'equilibrium parameter' or 'separation factor' R_L, defined by the following equation:

$$R_L = \frac{1}{1 + K_L C_0} \quad (11)$$

where C_0 is the initial dye concentration ($mg\,L^{-1}$) and K_L is the Langmuir constant ($L\,mg^{-1}$). It is generally accepted that R_L values indicate the type of isotherm, with an R_L value close to zero indicating favorable adsorption. At present, the R_L values were found to be close to zero for both dyes and dye concentrations C_0 in the range of 1.4–14 $mg\,L^{-1}$ for Methylene Blue and 3.2–32 $mg\,L^{-1}$ for Red Basic 22 (Table 3), for all adsorbents studied. Moreover, the higher R_L values of the untreated wheat straw indicate that adsorbent treatment enhanced adsorption properties and verifies the findings according to the Freundlich model.

Introducing the q_m parameter (in $mg\,g^{-1}$), as a variable, possibly depended on C_p, we observe an almost linear relation between them:

$$q_m = a_{qm} + b_{qm} C_p \quad (12)$$

By combining relations (2) and (12) we obtain Eq. (13), which simulates q_m parameter (in $mg\,g^{-1}$), growth as a function of the mild acid hydrolysis processing time, including preheating period >(40 + 30)/60 = 1.17 h:

$$q_m = q_{me} - (q_{me} - q_{m0})e^{-k_{qm}t} \quad (13)$$

where q_{me} is the value of q_m for $t \to \infty$, q_{m0} is the value of q_m for $t = 0$ (at the beginning of the preheating period) and k_{qm} is the kinetic constant in h^{-1}. The parameters were found by non-linear regression analysis (Table 6). The solid line for the Methylene Blue absorption and the dashed line for the Red Basic 22 adsorption on the fine grinded wheat straw fraction are shown in Fig. 5a. By the assumption that $k_{qm} = k_p$ then $q_{me} = a_{qm} + b_{qm}C_{pe}$, and $q_{m0} = q_{me} - b_{qm}C_{pe}$.

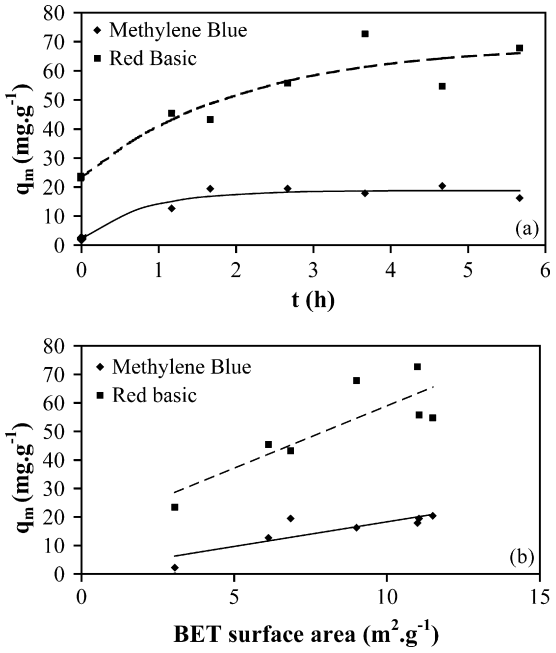

Fig. 5. Simulation of the Langmuir parameter (q_m in $mg\,g^{-1}$) vs. (a) the fine grinded wheat straw acid hydrolysis time (t in h) and (b) the corresponding BET surface area (B in $m^2\,g^{-1}$). The solid lines correspond to the methylene blue adsorption data and the dashed lines correspond to the Red Basic 22 adsorption data.

Alternatively, Eq. (13) comes from the combination of Eq. (3) with the following equation:

$$q_m = a'_{qm} + b'_{qm} B \quad (14)$$

by the assumption that $k_{qm} = k_B$. In this case $q_{me} = a'_{qm} + b'_{qm}B_e$, and $q_{m0} = q_{me} - b'_{qm}(B_e - B_0)$.

The results from the fitting of Eq. (14) to the experimental data are given in Fig. 5b (the solid line for the Methylene Blue absorption and the dashed line for the Red Basic 22 adsorption on the fine grinded wheat straw fraction) and the parameters' values (estimated by non-linear regression analysis) are given in Table 6. The q_m values are increasing linearly vs. BET surface area increasing for both (fine and coarse grinded) wheat straw fractions.

Untreated and hydrolyzed wheat straw were both found to adsorb Methylene Blue and Red Basic 22 strongly. The adsorption of Methylene Blue was stronger in comparison with the adsorption of Red Basic 22 by the same adsorbent, when parameter values are estimated according to the Freundlich isotherm, which is more consistent with multi-layer adsorption. The K_F values and the adsorption capacities (q_m), estimated using the Freundlich and the Langmuir models, respectively, indicate that the adsorption properties of the wheat straw were enhanced by mild acid hydrolysis. The time of mild acid hydrolysis was also found to affect adsorptivity, as noted by the difference in the values of K_F for the 0.5–5 h hydrolyzed material.

3.4. Kinetics of adsorption

The kinetics of adsorption of methylene blue on various materials have been extensively studied using various kinetic equations

[8,9,18,19,36–38]. The best prevailing equation is the Lagergren [39] one:

$$q - q_t = q e^{-kt} \quad (15)$$

where q and q_t are the amounts of dye adsorbed per unit mass of the adsorbent material (in mg g^{-1}) at equilibrium time (∞) and time t, respectively, while k is the first order rate constant for the adsorption process (in min^{-1}). In logarithmic form:

$$\ln(q - q_t) = \ln q - kt \quad (16)$$

The Lagergren equation can be rewritten as follows:

$$\frac{C_0 - C_e}{m} - \frac{C_0 - C}{m} = \frac{C_0 - C_e}{m} e^{-kt}$$

where C, C_0, C_e are the concentrations of methylene blue in the bulk solution at time t, 0, and ∞, respectively, while m is the weight of the adsorbent used (in g). Further modification gives:

$$C - C_e = (C_0 - C_e)e^{-kt} \quad (17)$$

and in logarithmic form:

$$\ln(C - C_e) = \ln(C_0 - C_e) - kt \quad (18)$$

The Lagergren plots of $\ln(q - q_t)$ vs. t for methylene blue on original wheat straw were found to be linear, indicating the first order nature of the adsorption process (Fig. 6). The values of the first order rate constants, the correlation coefficients (R-values) and the S.E.E. are given in Table 4.

All the linear correlations were found to be statistically significant, as is evident from both the R-values and the S.E.E.-values, indicating the applicability of this kinetic equation to the adsorption of methylene blue. The calculated first order rate constant value (k) of the Lagergren equation for the untreated wheat straw was found to be higher than that estimated for the hydrolyzed material for methylene blue and about the same for red basic 22. The results show that the pretreatment enhances the adsorption rate by increasing both the amount of dye adsorbed per unit mass of the adsorbent (q in mg g^{-1}) at equilibrium time ($t \to \infty$) but not the first order rate constant (k in min^{-1}) for the adsorption process. This enhancement can possibly be attributed to the removal of the hemicelluloses during sulfuric acid treatment (Table 1 and Fig. 1b), resulting in the 'opening' of the pores of the lignocellulosic matrix's structure and the increasing the BET surface area of the absorbent material (Table 1 and Fig. 2).

The rate constant value (k in min^{-1}) of the Lagergren equation is given in Fig. 7 for Methylene Blue adsorption on fine grinded wheat straw vs. hydrolysis time (t in h). Since the experimental data for k vs. t give a profile/path which is inverse to that obtained by Eqs. (4), (8) and (13), we tried fitting the following isomorphic (to these equations) relation with satisfactory results, judging by

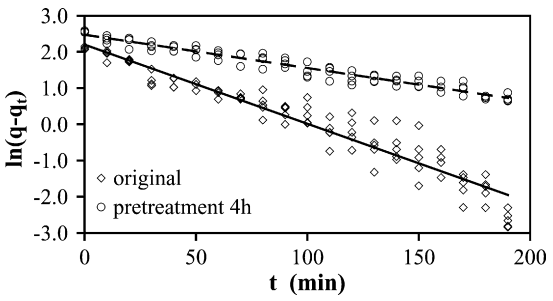

Fig. 6. Lagergren plots for the removal of methylene blue by adsorption on original and acid hydrolyzed for 4 h fine grinded wheat straw at 23 °C (C_0 = 14.0 mg L^{-1}).

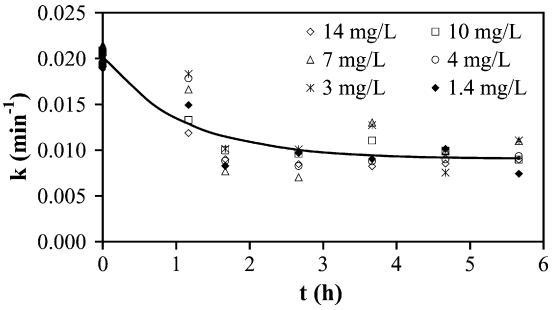

Fig. 7. The plot of k (Lagergren rate constant k in min^{-1}) for the removal of methylene blue by adsorption on original and acid hydrolyzed for 4 h fine grinded wheat straw vs. the acid hydrolysis time (hydrolysis conditions as in Fig. 1).

the low S.E.E.-value:

$$k = k_0 - (k_0 - k_e)e^{-k_k t} \quad (19)$$

where k_e is the value of k for hydrolysis time $t \to \infty$, k_0 is the value of k for t = 0 (at the beginning of the hydrolysis preheating period) and k_k is the kinetic constant in h^{-1}. The parameters' values were found by non-linear regression analysis: k_e = 0.0090 min^{-1}, k_0 = 0.0201 min^{-1}, k_k = 0.9084 h^{-1} and S.E.E. = 0.0020. This equation was found to be applicable only in the case of Methylene Blue adsorption; for Red Basic 22 the k parameter was practically not affected by the hydrolysis time.

According to the Lagergren model and the Arrhenius law $k = pe^{-E/RT}$, the activation energy for the adsorption of methylene blue on untreated and pre-treated wheat straw was estimated by plotting $\ln k$ (Lagergren rate constant k in min^{-1}) vs. $1/T$ (adsorption temperature T in K). The methylene blue adsorption activation energies E were found to be approximately equal to 2.5 kcal/mol (10.5 kJ/mol) for the hydrolyzed materials, significantly lower than the activation energy of the original material (3.6 kcal/mol or 15.1 kJ/mol).

Kinetic studies using the Lagergren equation provided values of k for the hydrolyzed material lower (in the case of fine grinded wheat straw) or similar (in the case of coarse grinded wheat straw) than those estimated for the original material under the same conditions. On the contrary, the adsorption rate for the hydrolyzed material (dC/dt or dq_t/dt) was higher than those estimated for the original material under the same conditions. This can be explain by the fact that $dC/dt\ d(C - C_e)/dt = -k(C - C_e)$ or $dq_t/dt = -d(q - q_t)/dt = k(q - q_t)$, i.e. dC/dt depends on both k (which does not increases), and the difference $(C - C_e)$ which increases (because C_e decreases for the hydrolyzed materials comparing to the untreated one, referring on the same dye initial concentration C_0). In the same way, dq_t/dt depends both on k and $(q - q_t)$ (which increases, because q increases for the hydrolyzed materials, referring on the same C_0).

3.4.1. Effect of stirring speed

Agitation is a classic parameter in sorption phenomena, influencing the distribution of the solute in the bulk solution and the formation of the external boundary film. The effect of stirring speed (in rpm) on the adsorption rate constant k (in min^{-1}) of the original material was studied. The kinetics seem to have been affected by the agitation speed for values between 0 and 500 rpm, thus confirming that the influence of external diffusion in the sorption kinetic control played a significant role. On the contrary, the slight effect of agitation for the range 600–1000 rpm indicates that external mass transfer was not the rate-limiting step, and implies that intraparticle diffusion resistance needs to be included in the analysis of overall sorption [8,9,18,19,36–38].

Table 4
Lagergren kinetic parameters of Methylene Blue adsorption on fine grinded wheat straw (23 °C).

C_0 (mg L^{-1})	Original wheat straw	Wheat straw pre-treated with 1.8 M H_2SO_4 at 100 °C					
		0.5 h[a]	1 h[a]	2 h[a]	3 h[a]	4 h[a]	5 h[a]
Methylene Blue							
Adsorption rate constant (k in min^{-1})							
14	0.0206	0.0119	0.0090	0.0085	0.0082	0.0085	0.0090
10	0.0208	0.0133	0.0100	0.0096	0.0110	0.0099	0.0090
7	0.0212	0.0166	0.0077	0.0070	0.0130	0.0099	0.0110
4	0.0193	0.0178	0.0088	0.0083	0.0088	0.0090	0.0093
3	0.0199	0.0183	0.0101	0.0101	0.0127	0.0075	0.0111
1.4	0.0191	0.0149	0.0083	0.0097	0.0090	0.0101	0.0074
Correlation coefficient (R)							
14	−0.9399	−0.9869	−0.9707	−0.9857	−0.9855	−0.9771	−0.9772
10	−0.9311	−0.9826	−0.9804	−0.9883	−0.9896	−0.9660	−0.9844
7	−0.9104	−0.9717	−0.9866	−0.9823	−0.9934	−0.9788	−0.9707
4	−0.8599	−0.9483	−0.9780	−0.9763	−0.9897	−0.9848	−0.9615
3	−0.7820	−0.9601	−0.9734	−0.9825	−0.9201	−0.9679	−0.9728
1.4	−0.6543	−0.8894	−0.9568	−0.9427	−0.9219	−0.9401	−0.9390
S.E.E. (mg L^{-1})							
14	0.71	0.48	0.48	0.48	0.57	0.72	0.57
10	0.57	0.47	0.39	0.36	0.41	0.60	0.41
7	0.43	0.46	0.23	0.29	0.26	0.44	0.27
4	0.74	0.37	0.18	0.23	0.21	0.17	0.21
3	0.57	0.22	0.15	0.16	0.16	0.19	0.15
1.4	0.44	0.10	0.10	0.14	0.15	0.16	0.12
Red Basic 22							
Adsorption rate constant (k in min^{-1})							
32	0.0047	0.0050	0.0030	0.0048	0.0069	0.0062	0.0056
22	0.0061	0.0056	0.0033	0.0053	0.0072	0.0073	0.0074
16	0.0080	0.0057	0.0038	0.0062	0.0087	0.0088	0.0118
10	0.0099	0.0086	0.0037	0.0055	0.0099	0.0108	0.0128
6	0.0076	0.0113	0.0060	0.0090	0.0106	0.0138	0.0078
3.2	0.0049	0.0096	0.0064	0.0059	0.0054	0.0074	0.0079
Correlation coefficient (R)							
32	−0.9208	−0.9837	−0.9779	−0.9833	−0.9884	−0.9864	−0.9821
22	−0.9228	−0.9772	−0.9775	−0.9829	−0.9852	−0.9900	−0.9848
16	−0.9240	−0.9635	−0.9584	−0.9813	−0.9683	−0.9820	−0.9914
10	−0.8635	−0.9891	−0.9707	−0.9662	−0.9692	−0.9761	−0.9764
6	−0.8080	−0.9815	−0.9523	−0.9802	−0.9378	−0.9483	−0.9829
3.2	−0.6869	−0.9579	−0.9341	−0.9320	−0.8812	−0.9418	−0.9413
S.E.E. (mg L^{-1})							
32	1.43	0.84	0.71	0.84	0.99	1.11	1.08
22	1.01	0.73	0.55	0.62	0.79	0.75	0.83
16	0.76	0.67	0.54	0.45	0.71	0.52	0.49
10	1.91	4.35	3.14	5.13	1.86	2.61	1.54
6	1.98	1.83	1.93	1.89	1.78	1.23	1.65
3.2	1.53	1.51	2.02	1.75	1.52	1.63	1.50

3.4.2. Intra-particle diffusion model

The adsorbate species are most probably transported from the bulk of the solution into the solid phase through an intra-particle diffusion/transport process, which is frequently the rate-limiting step in many adsorption processes, especially in a rapidly stirred batch reactor. The possibility of intra-particle diffusion was explored by using the intra-particle diffusion model [9,11,18,20,34]:

$$q_t = k_p\sqrt{t} + c \quad (20)$$

where q_t is the amount of dye adsorbed at time t; c is the intercept and k_p is the intra-particle diffusion rate constant (in mg g^{-1} min$^{-0.5}$). The k_p values for Methylene Blue adsorption on original and 4 h hydrolyzed fine grinded wheat straw, were estimated by linear regression analysis, and found equal to 0.612 and 0.827 mg g^{-1} min$^{-0.5}$, respectively. The c-values were found 1.353 and 0.086 mg g^{-1}, respectively. The S.E.E.-values were found 0.655 and 0.693, respectively and the R-values were found 0.9601 and 0.9751, respectively, indicating the applicability of this model to the data. It is thereby proven that an intra-particle diffusion process takes place. The estimated values of k_p are found higher for hydrolyzed wheat straw than for the original material. The results show that the acid hydrolysis pretreatment enhances the adsorption rate by increasing the intra-particle diffusion rate constant k_p. This enhancement can be attributed to the removal of the hemicelluloses and amorphous cellulose fraction during sulfuric acid treatment, resulting in the 'opening' of the pores of the lignocellulosic matrix's structure and the increasing of the BET surface area of the absorbent material (Table 1). The values of intercept are related to the boundary layer thickness, i.e. the larger intercept-value for the original wheat straw indicates stronger boundary layer effect.

The removal of methylene blue by adsorption on various materials was found to be rapid in the initial period of contact time and then to become slow and stagnate with the increase in contact time. The possible mechanism for the removal of the cationic dye by adsorption is assumed to involve the following four steps [20]: (a) migration of dye from bulk of the solution to the surface of the adsorbent, (b) diffusion of dye through the boundary layer to the surface of the adsorbent, (c) intra-particle diffusion of dye into

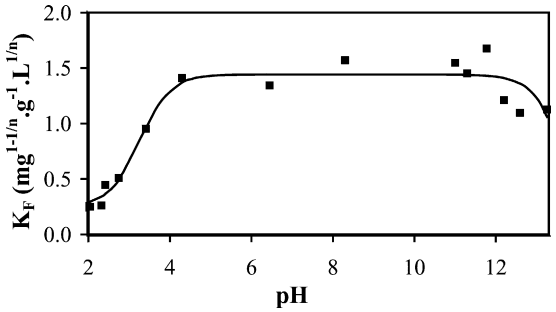

Fig. 8. Simulation of the Freundlich parameter values (K_F in $mg^{1-1/n}\,g^{-1}\,L^{1/n}$) for the removal of methylene blue by adsorption on original fine grinded wheat straw vs. initial pH of the dye solution at 23 °C.

the interior pores of the adsorbent particle, and (d) adsorption of dye at an active site on the surface of the adsorbent.

Since the uptake of the dye at the active sites of adsorbent is a rapid process, the rate of adsorption is mainly governed by either a liquid phase mass transfer rate or an intra-particle mass transfer rate [9,11,18–20,34]. In the present study it was found that the intra-particle diffusion model was sufficiently applicable, indicating that intra-particle mass transfer was the rate-determining step.

Moreover, the methylene blue adsorption activation energy for the pre-treated samples was found to be approximately 10.5 kJ/mol, significantly lower than the activation energy of the original material (15.1 kJ/mol). The fact that the activation energies were low strongly suggests that physical reaction was the controlling step of the adsorption process.

3.5. Effect of pH on adsorption

The effect of the pH of the dye solution on the amount of dye adsorbed was studied by varying the initial pH under constant process conditions. The following equation was developed [36] to simulate the effect of pH on the Freundlich parameter K_F of adsorption isotherms of Methylene Blue adsorption on beech sawdust:

$$K_F = \frac{\gamma_1}{1 + e^{\alpha_1 - \beta_1\,\mathrm{pH}}} - \delta_1 \times 10^{-(14-\mathrm{pH})} + \varepsilon_1 \tag{21}$$

where α_1, β_1, γ_1, δ_1, ε_1 are empirical parameters. The parameter δ_1 was set equal to zero for the range of pH 1.7–8.0 (the pH of the dye solutions were adjusted using dilute H_2SO_4 solution) and estimated from the experimental data for the range of pH 8.0 to 13.0 (the pH of the dye solutions were adjusted using dilute NaOH solution). Eq. (21) simulation results of the Freundlich parameter values (K_F in $mg^{1-1/n}\,g^{-1}\,L^{1/n}$) for the removal of Methylene Blue by adsorption on original fine grinded wheat straw vs. initial pH of the dye solution at 23 °C are presented in Fig. 8. The corresponding simulation parameter values are:

$$\alpha_1 = 7.81, \quad \beta_1 = 2.63, \quad \gamma_1 = 1.19, \quad \delta_1 = 4.21, \quad \varepsilon_1 = 0.25,$$

$$\text{S.E.E.} = 0.169$$

The K_F values were significantly lower for pH values between 1.5 and 4 for the untreated and the pre-treated materials. The lower adsorption of methylene blue at acidic pH is due to the presence of excess H^+ ions that compete with the dye cation for adsorption sites. As the pH of the system increases, the number of available positively charged sites decreases while the number of the negatively charged sites increases. The negatively charged sites favor the adsorption of dye cation due to electrostatic attraction. The increase in initial pH from 8 to 13 did not increase the amount of dye adsorbed. The K_F values were a little lower for pH values between 12 and 13 for the untreated and the pre-treated materials due to the transformation of methylene blue. The final pH of the solution was found to decrease only slightly (by 0.3–0.5 pH units) after adsorption of methylene blue (in cationic form) with the release of H^+ ions from the active sites of the adsorbent surface. The results are generally in agreement with the other literature reports [8,9,18–20,38].

3.6. Column studies

Oulman [40] proposed the use of a bed depth service model for simulating GAC (granular activated carbon) adsorption beds. The model, first developed by Bohart and Adams [41], was based on surface reaction theory and is equivalent to the logistic curve [18,19,42–48]. The Bohart–Adams equation is as follows:

$$\ln\left(\frac{C_i}{C} - 1\right) = \frac{KNx}{u} - KC_i t \tag{22}$$

in which C = effluent concentration ($mg\,L^{-1}$); C_i = influent concentration ($mg\,L^{-1}$); K = an adsorption rate coefficient ($L\,mg^{-1}\,min^{-1}$); N = an adsorption capacity coefficient ($mg\,L^{-1}$); x = bed depth (cm); u = linear velocity ($cm\,min^{-1}$); and t = time (min). The above equation can be rewritten as

$$\frac{C}{C_i} = \frac{1}{1 + e^{a-bt}} \tag{23}$$

where $a = KNx/u$ and $b = KC_i$.

Eq. (23) corresponds to the 'logistic curve', an S-shaped curve, which is symmetrical around its midpoint at $t = a/b = (Nx)/(uC_i)$, $C = C_i/2$. One of the limitations of the 'simple logistic function' is that it requires symmetry. However, many breakthrough curves are not perfectly symmetrical, owing to the nature of the adsorption system under study. Clark [44] has developed an alternative to the 'simple logistic function', called the 'generalized logistic function', which incorporates the parameter n of the Freundlich adsorption isotherm:

$$C = \left[\frac{C_i^{n-1}}{(1 + Ae^{-rt})}\right]^{\frac{1}{n-1}} \tag{24}$$

where n = inverse of the slope of the Freundlich isotherm; $A = e^a$; $r = b$.

Eq. (24) was applied to the effluent data from the column adsorber (Fig. 7). Transforming Eq. (24):

$$\left(\frac{C_i}{C}\right)^{n-1} - 1 = Ae^{-rt} \tag{25}$$

Linearizing Eq. (25):

$$\ln\left[\left(\frac{C_i}{C}\right)^{n-1} - 1\right] = \ln A - rt \tag{26}$$

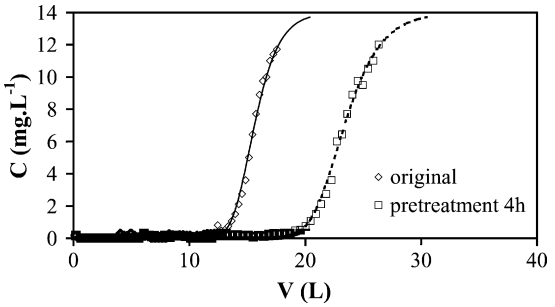

Fig. 9. Breakthrough curves for fixed beds of original (solid line) and hydrolyzed for 4 h fine grinded wheat straw (dashed line). Methylene blue solution flow rate 10 mL/min and bed height 10 cm.

Table 5
Estimated parameter values for Methylene Blue (C_i = 14 mg L^{-1}) and Red Basic 22 (C_i = 32 mg L^{-1}) adsorption according to the Bohart–Adams bed depth service model.

Parameter	Original wheat straw	Wheat straw pre-treated with 1.8 M H_2SO_4 at 100 °C					
		0.5 h[a]	1 h[a]	2 h[a]	3 h[a]	4 h[a]	5 h[a]
Fine grinded wheat straw							
Methylene Blue							
Adsorption rate coefficient (K in mg^{-1} L min^{-1})	0.00031	0.00040	0.00045	0.00038	0.00050	0.00029	0.00063
Adsorption capacity coefficient (N in mg L^{-1})	5123	6028	6697	7367	7098	7887	7833
Correlation coefficient (R)	−0.9752	−0.9264	−0.9919	−0.9423	−0.9212	−0.9697	−0.9048
S.E.E. (mg g^{-1})	0.371	0.408	0.581	0.639	0.719	0.654	0.402
Red Basic 22							
Adsorption rate coefficient (K in mg^{-1} L min^{-1})	0.00030	0.00041	0.00043	0.00027	0.00026	0.00019	0.00027
Adsorption capacity coefficient (N in mg L^{-1})	3480	6054	6726	7399	6936	7301	7290
Correlation coefficient (R)	−0.9910	−0.9414	−0.9643	−0.9161	−0.9323	−0.9814	−0.9784
S.E.E. (mg g^{-1})	1.056	1.161	0.946	1.041	1.026	0.932	0.843
Coarse grinded wheat straw							
Methylene Blue							
Adsorption rate coefficient (K in mg^{-1} L min^{-1})	0.00037	0.00037	0.00035	0.00035	0.00033	0.00027	0.00036
Adsorption capacity coefficient (N in mg L^{-1})	928	1052	1169	2341	2532	2813	2977
Correlation coefficient (R)	−0.9746	−0.9259	−0.9737	−0.9250	−0.9185	−0.9669	−0.9449
S.E.E. (mg g^{-1})	0.488	0.537	0.604	0.664	0.866	0.787	0.571
Red Basic 22							
Adsorption rate coefficient (K in mg^{-1} L min^{-1})	0.00036	0.00037	0.00033	0.00024	0.00017	0.00017	0.00015
Adsorption capacity coefficient (N in mg L^{-1})	630	1056	1174	2351	2474	2605	2771
Correlation coefficient (R)	−0.9578	−0.9099	−0.9650	−0.9167	−0.9020	−0.9495	−0.9517
S.E.E. (mg g^{-1})	1.389	1.528	0.984	1.082	1.235	1.123	1.197

[a] Hydrolysis reaction time without including preheating time.

The values of A and r can be thus estimated from the column effluent data assuming C_i = column influent and C = the column effluent at time t. As can be observed in Fig. 9, the theoretical estimations–curves according to the theoretical model expressed by Eq. (24)—sufficiently simulate the experimental data. In addition, the adsorption rate coefficient (K) and the adsorption capacity coefficient (N), shown in Table 5, were estimated from the A and r-values. The adsorption capacity coefficient values were found to be higher for the hydrolyzed materials than for the original one (Fig. 10a–d).

Introducing the N parameter (in mg L^{-1}), as a variable, possibly depended on C_p, we observe an almost linear relation between them:

$$N = a_N + b_N C_p \tag{27}$$

By combining relations (2) and (27) we obtain Eq. (28), which simulates N parameter (in mg L^{-1}), growth as a function of the mild acid hydrolysis processing time, including preheating period

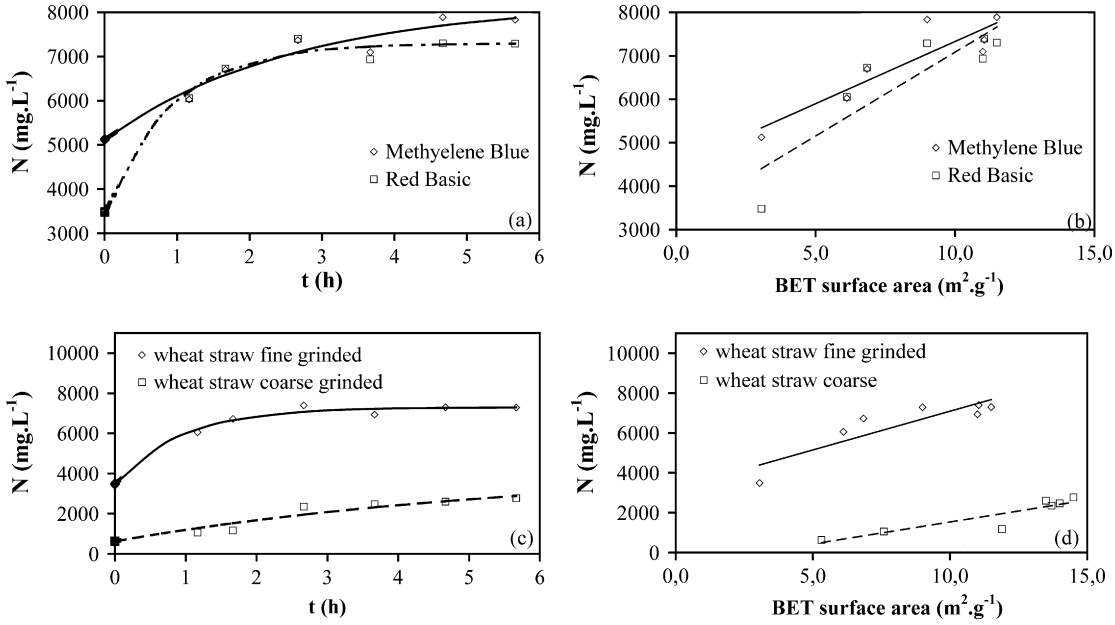

Fig. 10. Simulation of the Bohart–Adams equation adsorption capacity coefficient (N in mg L^{-1}) vs. (a) the fine grinded wheat straw acid hydrolysis time (t in h), (b) the hydrolyzed fine grinded wheat straw BET surface area (B in m^2 g^{-1}), (c) the wheat straw acid hydrolysis time and (d) the hydrolyzed wheat straw BET surface area. In (a) and (b) the solid and the dashed lines correspond to the Methylene Blue and Red Basic 22 adsorption data, respectively. In (c) and (d) the solid and the dashed lines correspond to the Red Basic 22 adsorption data on fine grinded and coarse grinded wheat straw, respectively.

Table 6
The simulation parameters of the removed polysaccharides C_p, the BET surface area, the K_F values, the adsorption capacities (q_m) and the adsorption capacity coefficient values (N).

Simulation parameters	Fine grinded wheat straw		Coarse grinded wheat straw	
	Methylene Blue	Red Basic 22	Methylene Blue	Red Basic 22
Simulation of the removed polysaccharides C_p vs. t				
C_{pe}	38.81%		38.33%	
k_p	0.879		0.910	
S.E.E.	1.74%		0.91%	
Simulation of the BET surface area B				
B vs. hydrolysis time t				
B_0	3.06		5.31	
B_e	12.63		19.13	
k_B	0.332		0.224	
S.E.E.	1.78		1.79	
B vs. removed polysaccharides C_p				
b_B	20.29		24.03	
a_B	2.52		4.36	
Correlation coefficient (R)	0.8679		0.9335	
Simulation of the Freundlich K_F values				
K_F vs. hydrolysis time t				
K_{F0}	1.57	3.02	2.68	5.17
K_{Fe}	10.86	8.90	14.62	11.95
k_{KF}	1.07	1.13	1.27	1.40
S.E.E.	1.47	0.64	3.40	2.06
K_F vs. BET surface area B				
b'_{KF}	24.81	15.49	32.45	18.30
a'_{KF}	1.63	3.18	2.56	5.21
Correlation coefficient (R)	0.9280	0.9564	0.8695	0.8502
Simulation of the Langmuir adsorption capacity q_m				
q_m vs. hydrolysis time t				
q_{m0}	2.23	23.39	3.82	40.00
q_{me}	18.80	68.99	25.37	111.67
k_{qm}	1.27	0.49	1.56	0.25
S.E.E.	2.45	8.04	6.09	16.55
q_m vs. BET surface area B				
b'_{qm}	1.73	4.40	2.12	4.40
a'_{qm}	1.00	15.08	−2.87	15.08
Correlation coefficient (R)	0.8539	0.8403	0.8085	0.8403
Simulation of the Bohart–Adams adsorption capacity coefficient values N				
N vs. hydrolysis time t				
N_0	5123	3480	928	630
N_e	8231	7300	18723	4316
k_N	0.380	1.067	0.023	0.167
S.E.E.	270	231	346	304
N vs. BET surface area B				
b'_N	287	388	214	223
a'_N	4464	3205	−487	−693
Correlation coefficient (R)	0.9014	0.8818	0.8659	0.9121

>(40 + 30)/60 = 1.17 h:

$$N = N_e - (N_e - N_0)e^{-k_N t} \quad (28)$$

where N_e is the value of N for $t \to \infty$, N_0 is the value of N for $t = 0$ (at the beginning of the preheating period) and k_N is the kinetic constant in h^{-1}. The parameters of Eq. (27) were found by non-linear regression analysis (Table 6). The solid line is for the Methylene Blue absorption and the dashed line for the Red Basic 22 adsorption on the fine grinded wheat straw fraction in Fig. 10a and on the coarse grinded wheat straw fraction in Fig. 10c, respectively. By the assumption that $k_N = k_p$ then $N_e = a_N + b_N C_{pe}$, and $N_0 = N_e - b_N C_{pe}$.

Alternatively, the above Eq. (28) comes from the combination of Eq. (3) with the following equation:

$$N = a'_N + b'_N B \quad (29)$$

by the assumption that $k_N = k_B$. In this case $N_e = a'_N + b'_N B_e$, and $N_0 = N_e - b'_N(B_e - B_0)$.

The results from the fitting of Eq. (29) to the experimental data are given in Fig. 10b and d. The solid line presented in Fig. 10b is for the Methylene Blue absorption and the dashed line for the Red Basic 22 adsorption on the fine grinded wheat straw fraction. The solid line in Fig. 10d is for the Methylene Blue absorption and the dashed line for the Red Basic 22 adsorption on the coarse grinded wheat straw fraction. Eq. (29) parameters' values estimated with linear regression analysis are given in Table 6. The N values are increasing linearly vs. BET surface area increasing for both (fine and coarse grinded) wheat straw fractions.

Applying the bed depth service model for the simulation of straw adsorption beds, the adsorption capacity coefficient (N) values were found to be higher for the hydrolyzed wheat straw than for the original one. In addition, the linear correlations of the K_F values, the adsorption capacities (q_m) and the adsorption capacity coefficient values (N) vs. BET surface area were found to be statistically significant, as is evident from the correlation coefficient R-values presented in Table 6.

Mild acid hydrolysis is commonly employed in various processes owing to the simplicity, the safety in operation, the effectiveness and the inexpensive equipment/materials required (sulphuric acid might be also provided by treating spent acid released by nearby industrial units according to the principles of Industrial Ecology). The resulting adsorbent is a suitable low cost material that can be used as an alternative to commercial activated carbons for the removal of basic dyes from water/wastewater effluents. Economies arise when the facility that can use such adsorption materials is near a source of a lignocellulosic waste as agricultural residues, thus saving transportation cost and contributing to industrial ecology at local level.

4. Conclusions

The batch and column kinetics of Methylene Blue and Red Basic 22 adsorption on acid hydrolyzed wheat straw were simulated herein, using untreated wheat straw as control, in order to facilitate its potential use as a low cost adsorbent for wastewater dye removal. The simulation results indicate that mild acid hydrolysis of the wheat straw enhanced its adsorption properties considerably. This can be attributed to the 'opening' of the pores of the structure of the lignocellulosic substrate and the increasing of the BET surface area of the absorbent material by the removal of the hemicelluloses and the amorphous part of cellulose. The linear correlation of the BET surface area vs. the removed by the acid hydrolysis polysaccharides (cellulose and hemicelluloses) fraction was found to be statistically significant. Moreover, the linear correlations of the K_F values, the adsorption capacities (q_m) and the adsorption capacity coefficient (N) values vs. the BET surface area, were also found to be statistically significant, allowing good predictability for industrial applications.

Acknowledgment

The authors thank the Research Center of the University of Piraeus for the financial support.

References

[1] G. Crini, Non-conventional low-cost adsorbents for dye removal: a review, Bioresour. Technol. 97 (9) (2006) 1061–1085.
[2] A. Shukla, Y.-H. Zhang, P. Dubey, J.L. Margrave, The role of straw in the removal of unwanted materials from water, J. Hazard. Mater. B95 (2002) 137–152.
[3] V.J.P. Poots, G. McKay, J.J. Healy, Removal of basic dye from effluent using wood as an adsorbent, J. Wat. Poll. Contr. Fed. 50 (5) (1978) 926–935.
[4] P. Nigam, G. Armour, I.M. Banat, D. Singh, R. Marchant, Physical removal of textile dyes from effluents and solid-state fermentation of dye-adsorbed agricultural residues, Bioresour. Technol. 72 (2000) 219–226.
[5] S.I. Abo-Elela, M.A. el-Dib, Color removal via adsorption on wood shaving, Sci. Tot. Environ. 66 (1987) 269–273.
[6] O. Hamdaoui, Batch study of liquid-phase adsorption of methylene blue using cedar sawdust and crushed brick, J. Hazard. Mater. 135 (1–3) (2006) 264–273.
[7] B.G.P. Kumar, L.R. Miranda, M. Velan, Adsorption of Bismark Brown dye on activated carbons prepared from rubberwood sawdust (*Hevea brasiliensis*) using different activation methods, J. Hazard. Mater. 126 (1–3) (2005) 63–70.
[8] C. Namasivayam, M.D. Kumar, R.A. Begum, 'Waste' coir pith—a potential biomass for the treatment of dyeing wastewaters, Biomass Bioenergy 21 (2001) 477–483.
[9] G. Annadurai, R.-S. Juang, D.-J. Lee, Use of cellulose based wastes for adsorption of dyes from aqueous solutions, J. Hazard. Mater. B92 (2002) 263–274.
[10] M.M. Nassar, Y.H. Magdy, Removal of different basic dyes from aqueous solutions by adsorption on palm-fruit bunch particles, Chem. Eng. J. 66 (1997) 223–226.
[11] M.M. Nassar, Intra-particle diffusion of basic red and basic yellow dyes on palm fruit bunch, Wat. Sci. Technol. 40 (7) (1999) 133–139.
[12] V.K. Garg, R. Gupta, A.-B. Yadav, R. Kumar, Dye removal from aqueous solutions by adsorption on treated straw, Bioresour. Technol. 89 (2003) 121–124.
[13] N.A. Ibrahim, A. Hashem, M.H. Abou-Shosha, Animiation of wood straw for removing anionic dyes from aqueous solutions, Polym. Plast. Technol. Eng. 36 (6) (1997) 963–971.
[14] S. Xu, J. Wang, R. Wu, J. Wang, H. Li, Adsorption behaviors of acid and basic dyes on crosslinked amphoteric starch, Chem. Eng. J. 117 (2) (2006) 161–167.
[15] C. Namasivayam, R. Radhika, S. Suba, Uptake of dyes by a promising locally available agricultural solid waste: coir pith, Waste Manage. 21 (2001) 381–387.
[16] W.T. Tsai, C.Y. Chang, M.C. Lin, S.F. Chien, H.F. Sun, M.F. Hsieh, Adsorption of acid dye onto activated carbons prepared from agricultural waste bagasse by $ZnCl_2$ activation, Chemosphere 45 (2001) 51–58.
[17] S.J. Allen, Q. Gan, R. Matthews, P.A. Johnson, Comparison of optimised isotherm models for basic dye adsorption by kudzu, Bioresour. Technol. 88 (2003) 143–152.
[18] F.A. Batzias, D.K. Sidiras, Dye adsorption by prehydrolysed beech sawdust in batch and fixed-bed systems, Bioresour. Technol. 98 (2007) 1208–1217.
[19] F.A. Batzias, D.K. Sidiras, Dye adsorption by calcium chloride treated beech sawdust in batch and fixed-bed systems, J. Hazard. Mater. B114 (1–3) (2004) 167–174.
[20] N. Kannan, M.M. Sundaram, Kinetics and mechanism of removal of methylene blue by adsorption on various carbons—a comparative study, Dyes Pigments 51 (2001) 25–40.
[21] D.K. Sidiras, E.G. Koukios, Acid hydrolysis of ball milled straw, Biomass 19 (4) (1989) 289–306.
[22] D.K. Sidiras, Simulation of dilute acid hydrolysis of lignocellulosic materials: wheat straw, Cell Chem. Technol. 32 (5–6) (1998) 405–425.
[23] L. Segal, J.J. Greely, A.E. Martin, C.M. Conrad, An empirical method for estimating the degree of crystallinity of native cellulose using the x-ray diffractometer, Textile Res. J. 29 (1959) 786–795.
[24] J.F. Saeman, J.F. Bubl, E.E. Harris, Quantitative saccharification of wood and cellulose, Ind. Eng. Chem. Anal. Ed. 17 (1945) 35–37.
[25] M. Somogyi, Notes on sugar determination, J. Biol. Chem. 195 (1952) 19–23.
[26] DIN 66132, Determination of specific surface area of solids by adsorption of nitrogen; single-point differential method according to Haul and Dümbgen (1975).
[27] N. Mosier, C. Wyman, B. Dale, R. Elander, Y.Y. Lee, M. Holtzapple, M. Ladisch, Features of promising technologies for pretreatment of lignocellulosic biomass, Bioresour. Technol. 96 (6) (2005) 673–686.
[28] B.P. Lavarack, G.J. Griffin, D. Rodman, The acid hydrolysis of sugarcane bagasse hemicellulose to produce xylose, arabinose, glucose and other products, Biomass Bioenergy 23 (5) (2002) 367–380.
[29] H.M.F. Freundlich, Über die adsorption in lösungen, Zeitschrift für Physikalische Chemie 57 (1906) 385–471.
[30] I. Langmuir, The constitution and fundamental properties of solids and liquids, J. Am. Chem. Soc. 38 (1916) 2221–2295.
[31] G. McKay, B.A. Duri, Simplified model for the equilibrium adsorption of dyes from mixtures using activated carbon, Chem. Eng. Proc. 22 (3) (1987) 145–156.
[32] V. Meshko, L. Markovska, M. Mincheva, A.E. Rondrigues, Adsorption of basic dyes on granular activated carbon and natural zeolite, Wat. Res. 35 (14) (2001) 3357–3366.
[33] G.M. Walker, L.R. Weatherley, Adsorption of dyes from aqueous solution—the effect of adsorbent pore size distribution and dye aggregation, Chem. Eng. J. 83 (2001) 201–206.
[34] S.V. Mohan, N.C. Rao, J. Karthikeyan, Adsorption removal of direct azo dye from aqueous phase onto coal based sorbents: a kinetic and mechanistic study, J. Hazard. Mater. B90 (2002) 189–204.
[35] F. Carrillo, M.J. Lis, J. Valldeperas, Sorption isotherms and behaviour of direct dyes on lyocel fibres, Dyes Pigments 53 (2002) 129–136.
[36] F.A. Batzias, D.K. Sidiras, Simulation of dye adsorption by beech sawdust as affected by pH, J. Hazard. Mater. 141 (2007) 668–679.
[37] F.A. Batzias, D.K. Sidiras, Wastewater treatment with gold recovery through adsorption by activated carbon, water pollution IV: modelling, measuring and prediction, in: C.A. Brebbia, (Ed.), Series: Progress in Water Resources, WIT Press, Southampton, vol. 3, 2001, pp. 143–152.
[38] F.A. Batzias, D.K. Sidiras, Optimal design of adsorption tower equipped with a novel packed biomass bed for colouring-processes-wastewater treatment, CHISA 2004, in: Proceedings of the 16th International Congress of Chemical & Process Engineering, Prague, Czech Republic, 2004, pp. 2705–2724.
[39] S. Lagergren, Zur theorie der sogenannten adsorption gelöster stoffe. Kungliga Svenska Vetenskapsakademiens, Handlingar 24 (1898) 1–39.
[40] C.S. Oulman, Logistic curve as a model for carbon bed design, J. Am. Wat. Works Assoc. 72 (1) (1980) 50–53.
[41] G.S. Bohart, E.Q. Adams, Adsorption in columns, J. Chem. Soc. 42 (1920) 523–544.
[42] R.A. Hutchins, New method simplifies design of activated-carbon systems, Chem. Eng. 80 (19) (1973) 133–138.
[43] B.M. Van Vliet, W.J. Weber, Comparative performance of synthetic adsorbents and activated carbon for specific compound removal from wastewaters, J. Wat. Pollut. Contr. Fed. 53 (11) (1981) 1585–1598.

[44] R.M. Clark, Modeling TOC removal by GAC: the general logistic function, J. Am. Wat. Works Assoc. 79 (1) (1987) 33–131.
[45] K.S. Low, C.K. Lee, A.Y. Ng, Column study on the sorption of Cr(IV) using quaternized rice hull, Bioresour. Technol. 68 (1999) 205–208.
[46] G.M. Walker, L.R. Weatherley, COD removal from textile industry effluent: pilot plant studies, Chem. Eng. J. 84 (2001) 125–131.
[47] U. Kumar, M. Bandyopadhyay, Fixed bed column study for Cd(II) removal from wastewater using treated rice husk, J. Hazard. Mater. B129 (1–3) (2006) 253–259.
[48] A. Cambiella, E. Ortea, G. Ríos, J.M. Benito, C. Pazos, J. Coca, Treatment of oil-in-water emulsions: performance of a sawdust bed filter, J. Hazard. Mater. B131 (1–3) (2006) 195–199.